

A polarization-modulation method for the near-field mapping of laterally grown InGaN samples.

Ruggero Micheletto^{1(*)}, Daisuke Yamada¹, Maria Allegrini² and Yoichi Kawakami¹

¹*Kyoto University, Graduate School of Engineering, Department of Electronic Science, Nishigyo-ku, Katsura, 615-8510 Kyoto, Japan*

²*Department of Physics "E. Fermi", University of Pisa and polyLAB-CNR, Largo Pontecorvo 3, 56127 Pisa, Italy*

(*)*Current address: Yokohama City University, International College of Art and Science, Division of Science, Basic and Applied Sciences, Seto 22-2, Kanazawa-ku, 236-0027 Yokohama, Japan*

ruggero.micheletto@optomater.kuee.kyoto-u.ac.jp

Abstract: Epitaxial Laterally overgrown (ELOG) InGaN materials are investigated using a polarization modulated scanning near-field optical microscope. The authors found that luminescence has spatial inhomogeneities and it is partially polarized. Near-field photoluminescence shows polarization phase fluctuation up to 45 degrees over adjacent domains. These results point toward the existence of asymmetries in carrier confinement due to structural anisotropic strain within the framework of the ELOG structure.

© 2008 Optical Society of America

OCIS codes: (250.5230) Photoluminescence; (180.4243) Near-field microscopy; (130.5990) Semiconductors; (240.5440) Polarization-selective devices

References and links

1. S. Nakamura, "The roles of structural imperfections in InGaN-based blue light emitting diodes and Lasers Diodes," *Science* **281**, 956–961 (1998).
2. A. Usui, H. Sunakawa, A. Sakai, and A. A. Yamaguchi, "Thick GaN epitaxial growth with low dislocation density by hydride vapor phase epitaxy," *Jpn. J. Appl. Phys.* **36**, L899–L902 (1997).
3. T. S. Zheleva, O. H. Nam, M. D. Bremser, and R. F. Davis, "Dislocation density reduction via lateral epitaxy in selectively grown GaN structures," *Appl. Phys. Lett.* **71**, 2472–2474 (1997).
4. M. D. Craven, S. H. Lim, F. Wu, J. S. Speck, and S. P. DenBaars, "Threading dislocation reduction via laterally overgrown nonpolar (11 $\bar{2}$) a-plane GaN," *Appl. Phys. Lett.* **81**, 1201–1203 (2002).
5. O. Stier, M. Grundmann, and D. Bimberg, "Electronic and optical properties of strained quantum dots modeled by 8-band k center dot p theory," *Phys. Rev. B* **59**, 5688–5701 (1999).
6. M. Matthews, J. Hsu, S. Gu, and T. Kuech, "Carrier density imaging of lateral epitaxially overgrown GaN using scanning confocal Raman microscopy," *Appl. Phys. Lett.* **79**, 3086–3088 (2001).
7. J. Hsu, M. Matthews, D. Abusch-Magder, R. Kleiman, D. Lang, S. Richter, S. Gu, and T. Kuech, "Spatial variation of electrical properties in lateral epitaxially overgrown GaN," *Appl. Phys. Lett.* **79**, 761–763 (2001).
8. A. Kaneta, M. Funato, Y. Narukawa, T. Mukai, and Y. Kawakami, "Direct correlation between nonradiative recombination centers and threading dislocations in InGaN quantum wells by near-field photoluminescence spectroscopy," *Phys. Status Solidi C* **3**, 1897–1901 (2006).
9. R. Micheletto, Y. Kawakami, C. Manfredotti, Y. Garino, and M. Allegrini, "Dichroism of diamond grains by a polarization modulated near field optical setup," *Appl. Phys. Lett.* **89**, 121125 (2006).
10. P. G. Gucciardi, M. Allegrini, R. Micheletto, T. Kotani, T. Hatada, and Y. Kawakami, "Waveguide behavior of Distributed Bragg Reflectors probed by polarization-modulated near-field optical microscopy," *J. Korean Phys. Soc.* **47**, S101–S108 (2005).

11. B. Bhushan and H. Fuchs, eds., *Applied Scanning Probe Methods II: Scanning Probe Microscopy Techniques* (Springer, 2005).
12. R. Micheletto, M. Allegrini, and Y. Kawakami, "Artifacts in Polarization Modulation Scanning Near-field Optical Microscopes," *J. Opt. A* **9**, 431–434 (2007).
13. S. Mononobe and M. Ohtsu, "Development of a fiber used for fabricating application oriented near-field optical probes," *IEEE Photon. Technol. Lett.* **10**, 99–101 (1998).
14. S. Mononobe, M. Naya, T. Saiki, and M. Ohtsu, "Reproducible fabrication of a fiber probe with a nanometric protrusion for near-field optics," *Appl. Opt.* **36**, 1496–1500 (1997).
15. T. Matsumoto, T. Ichimura, T. Yatsui, M. Kourogi, T. Saiki, and M. Ohtsu, "Fabrication of a near-field optical fiber probe with a nanometric metallized protrusion," *Opt. Rev.* **5**, 369–373 (1998).

Wide-band-gap group III nitride materials were used to make electronic and optical devices, such as LED and solid state Lasers[1]. One problem in the fabrication of these devices is the high density (10^9 - 10^{11} cm^{-2}) of threading dislocations (TDs) produced when the nitride materials are grown on lattice-mismatch substrates. One method to reduce TDs is to use a technique called Epitaxial Lateral Overgrowth (ELOG), a commonly used method that alters the growth orientation along striped regions of the sample[2, 3, 4].

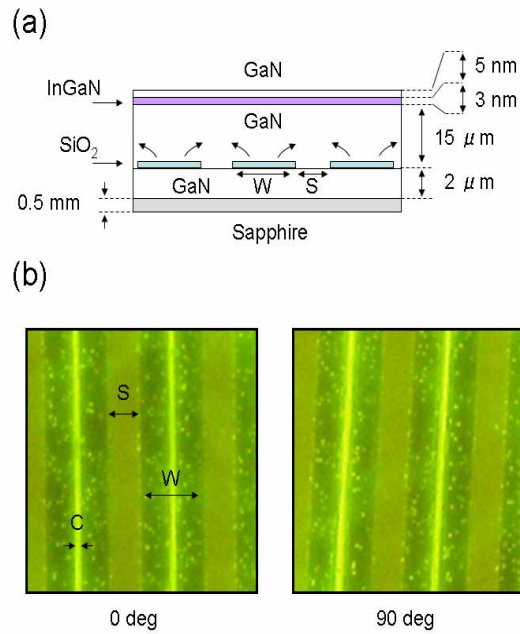


Fig. 1. (a) The structure of the ELOG samples tested. The arrows show the growth orientation in the proximity of the SiO_2 mask. Non-masked regions are indicated with the letter "S" (seed), and the remaining areas where lateral growth occurs are named "W" (wings). (b) Two PL $40 \times 40 \mu\text{m}$ images taken with a fluorescence optical microscope with excitation wavelength $\lambda=405\text{nm}$. The striped SiO_2 structure is evident with its bright boundary between two adjacent wings domains marked as "C". Image is focused on the mask plane $15 \mu\text{m}$ below surface. A number of brighter dots are noticeable in the wing region, these are inhomogeneities in the glass mask. Images are taken through polars oriented at 0 and 90 degrees. No appreciable contrast difference is observed, indicating that the polarization properties in far-field are very small.

This growth method is inherently anisotropic and induces the formation of stress in the crystal structure which may produce irregular carrier confinement features that are invisible to standard microscopy and are generally difficult to study. Since models point out that anisotropic strain induces asymmetry in the carrier localization and this results in polarized PL emission[5], we propose here a simple optical polarization modulation near-field technique to investigate on carrier confinement processes by studying the local polarization properties in the proximity of the sample surface.

The ELOG device sample was grown by Nichia Corporation (Japan) with MOCVD methodology: exact growth condition are undisclosed, crystal structure is shown in Fig. 1(a). A base layer of $2\mu\text{m}$ thick GaN is grown on a sapphire substrate, then a 200nm thin striped pattern of SiO_2 is deposited. Each strip is about $16\mu\text{m}$ wide and the separation between each of them is $4\mu\text{m}$. This structure acts as a mask for a subsequent $15\mu\text{m}$ GaN deposition.

The growth is initially possible only on the GaN surface available between strips. From this region, named "seed", the growth expands laterally into "wings" that invade the SiO_2 mask region and eventually contact the adjacent fronts[6, 7]. The growth extends vertically for $15\mu\text{m}$ then a final 3nm Indium doped quantum well (QW) is grown with its 5nm capping layer as in standard (non-ELOG) GaN/InGaN samples. The $4\mu\text{m}$ wide "seed" region between the SiO_2 mask is thought to have a reduced number of TDs because of the different crystal orientation and direction of growth[8].

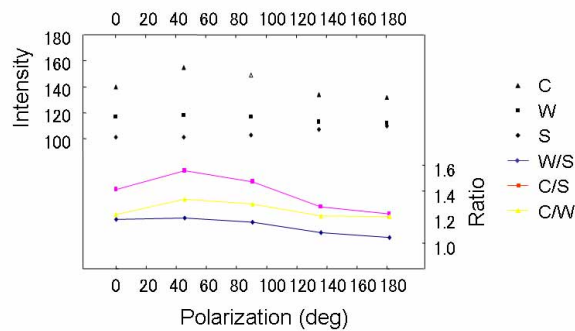


Fig. 2. The far-field dichroic properties of different growth domains in the crystal as described in table 1. Intensity is evaluated integrating regions of an 8 bit gray level image (RGB values are averaged) taken by a CCD camera mounted on a PL-optical microscope, see Table 1 for details.

In Fig. 1(b) we show two photoluminescence (PL) microscope images of the sample taken through polars (a Polaroid film) oriented at 0 and 90 degrees. The images are focused slightly below surface to show the mask structure clearly. No particular optical differences are appreciable. Focusing on the sample surface we imaged at 5 different polars angles, intensity measured in relevant areas are shown in table 1 and Fig. 2, confirming weak polarization effects in this far-field test.

There could be stronger confined fluctuations, local effects that are not detectable with a conventional far field microscope. We setup a home-made polarization-modulation system (PM-SNOM[9, 10, 11, 12]) capable of evaluating the polarization changing local properties of the sample. The apparatus is described in Fig. 3, a typical SNOM setup where a multiple-steps chemically etched 100nm apertured optical probe[13, 14, 15] is collecting the optical signal in the proximity of the surface of the sample. The incoming light that excites the photolumines-

Table 1. The far-field polarization relationship of different growth areas in the crystal. Intensity is evaluated taking PL-microscope pictures with a CCD camera and integrating the intensity of $2 \times 2 \mu\text{m}$ rectangles located in the "Seed", "Wing" and "C" domains. Small intensity variations related to the polarization angle can be observed. This dependence exists also among the shown intensity ratios proving slight dichroism phenomena between crystal domains. Measurements are taken focusing on the sample surface.

Angle	Seed	Wing	C	W/S	C/S	C/W
0	101	117	140	1.15	1.38	1.19
45	101	118	155	1.16	1.53	1.31
90	103	117	149	1.13	1.44	1.27
135	107	113	134	1.05	1.25	1.18
180	110	112	132	1.01	1.20	1.17

cence is a linearly polarized beam with variable polarization angle; this angle is continuously varied by filtering with a revolving polars film (frequency of rotation 63Hz). In this configuration, if the sample is not sensitive to polarization, fluorescence will be induced with same intensity on all angles; however, if there are birefringence or dichroic properties, the luminescence should produce intensity variations in tune with the modulation frequency. The lock-in amplifier will be able to generate a map of the sample dichroism and this map can be compared with the simultaneously taken photoluminescence map[12]. The natural residual birefringence of the probe will introduce a slight ellipticity of the light; a compensation of this disturbance is not required since the effect is the same everywhere on the sample (it is not position dependent). The effect appears simply as an offset value in the final maps.

The near-field luminescence map is shown in Fig. 4(a), the striped structure of the sample is noticeable with the "seed" and "wing" regions indicated. In (b) each pixel value represents the angular phase of the optical signal. The two maps (a) and (b) are taken simultaneously.

Domains and structures are different, indicating that we are free from cross-talk features[12]. Images are contrast-enhanced for visibility, however the strength of the dichroism can be calculated by treating the absolute signal values that are preserved in the actual data files and used with instrument calibration curves. The lock-in amplifier outputs the signal accordingly to its phase-voltage curve and subsequently an analog to digital (A/D) card converts this value to a unit labeled "counts" by the instrument. Lock-in response is linear with an inclination of about 16.9 deg per Volts, zero degree corresponds to zero volts. Our A/D converter responds also linearly with a sensitivity $\sigma_s = 562V_l + 2050$ where σ_s is in counts/Volts and V_l is the lock-in output in volts; with these parameters we can estimate easily the actual dichroism effect measured on each local feature mapped. The result of this is shown in the cross section of Fig. 5(b) along the lines r_1 and r_2 of Fig. 4 which are plotted with the corresponding phase shift values in *deg*.

We demonstrated strong polarization changing properties in the surface proximity of ELOG GaN/InGaN/GaN devices and we were able to obtain quantitative maps of the PL angular orientation. The investigation points toward the existence of peculiar asymmetries in carrier confinement; this suggests structural anisotropic strain within the polycrystalline framework of the ELOG structure. The technique used is applicable to organic conjugated materials as well as any optical absorbing or optical emitting films. It has an impact on all measurements where localized polarization properties of the optical emission are important. We would like to thank Dr. Akio Kaneta of Kyoto University for his help with sample description and preparation, we also acknowledge the Kyoto Nanotechnology cluster for support, the Italy-Japan bilateral Projects

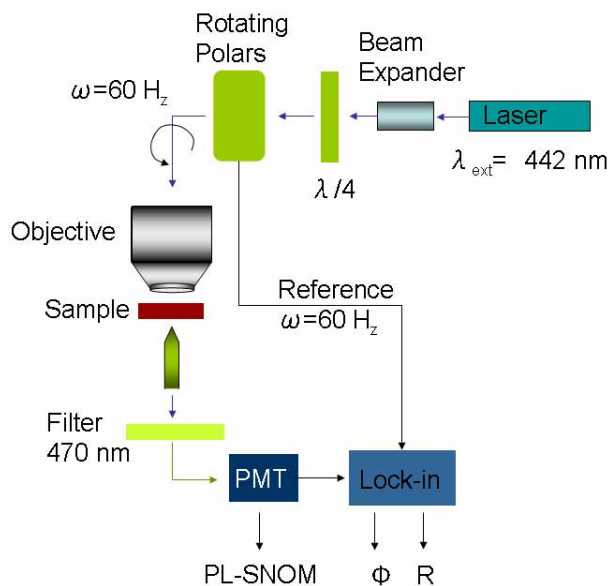


Fig. 3. The configuration of the PM-SNOM setup: a 442 nm Laser generates a beam of light that is expanded and circularly polarized by a $\lambda/4$ plate. A rotating polars film placed in front of the resulting beam linearizes the light, imposing an angle of orientation variable in time ($\omega \approx 60 \text{ Hz}$). This linearly polarized light excites the sample and induces photoluminescence. A near-field tip probes the sample, the resulting signal is collected by a photomultiplier (PM) and it is filtered by a lock-in amplifier tuned to the rotation frequency.

"2A2" and 31 "Near-field polarization contrast for nano-optics applications" for mobility support. We are indebted with Tatsuo Nakagawa of Unisoku Ltd, Osaka, for his assistance with the SNOM system and with A. La Barbera Translations, UK for support with English issues.

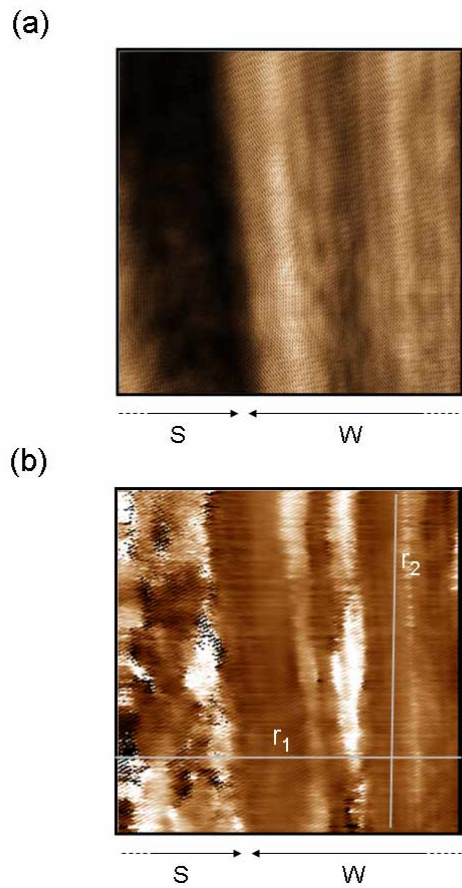
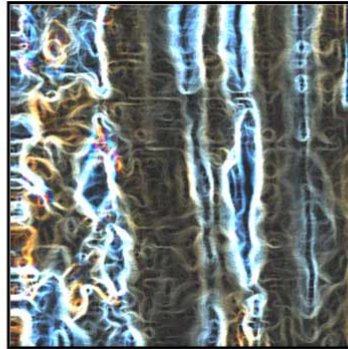


Fig. 4. Near field maps: (a) the photoluminescence is mapped locally with a 100nm apertured SNOM probe, image is $7.5 \times 7.5 \mu\text{m}$, intensity scale is arbitrary. (b) For every pixel of image (a) the polarization angle is reported in this map. "Seed" and "Wing" regions are indicated in the bottom of the images. Intensity scale in (b) represents the polarization phase as shown by the cross sections over r_1 and r_2 in Fig. 5(b).

(a)



(b)

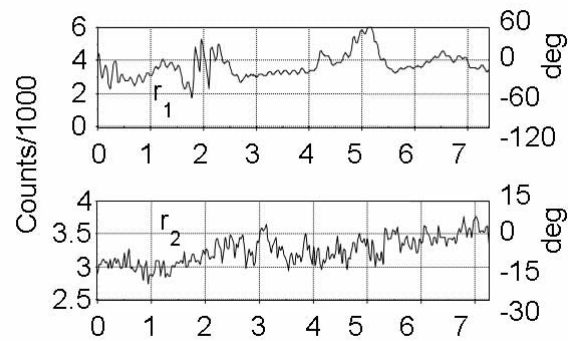


Fig. 5. Proximity phase properties of ELOG crystals: (a) the map in Fig. 4(b) is numerically treated to show phase differences, polarization is indefinite in "seed" regions whereas strong polarization changing effects are observed in the adjacent "wing" domain. The image is $7.5 \times 7.5 \mu\text{m}$. (b) Profiles with calibrated phase values corresponding to the cross sections r_1 and r_2 of Fig. 4.